

Phase morphology of injection-moulded polycarbonate/acrylonitrile-butadiene-styrene blends

M.-P. Lee, A. Hiltner* and E. Baer

Department of Macromolecular Science, and Center for Applied Polymer Research, Case Western Reserve University, Cleveland, OH 44106, USA

(Received 26 December 1990; revised 23 January 1991; accepted 27 January 1991)

The morphology of injection-moulded blends of polycarbonate (PC) and acrylonitrile-butadiene-styrene (ABS) has been examined across the entire composition range. Brittle fracture surfaces were etched to remove selectively the PC phase and viewed in the scanning electron microscope. Morphological features observed through the thickness of injection-moulded plaques were the basis for the identification of three composition ranges. In PC-rich blends, the ABS phase formed a bead-and-string structure oriented in the injection direction near the edge, while in the centre the ABS was dispersed as rubber domains and spherical particles of free styrene-acrylonitrile (SAN). A transition occurred between PC/ABS 70/30 and 60/40 wt% compositions from the bead-and-string structure with some interconnections to a coalesced, stratified morphology near the edge; while in the centre, the morphology changed from a dispersion of rubber particles and free SAN particles to thick coalesced ABS domains that created regions where ABS was co-continuous with PC. The ABS-rich blends had a conventional blend morphology with PC domains dispersed in ABS. Qualitatively, the solid-state morphology could be explained in terms of the melt morphology created by the melt flow pattern during mould filling, and subsequent relaxation during cooling prior to solidification.

(Keywords: acrylonitrile-butadiene-styrene; polycarbonate; blend morphology; injection moulding)

INTRODUCTION

Blending to achieve a microheterogeneous mixture of two or more polymers is a well known method used to improve mechanical, environmental and rheological properties of polymers. Since in these blends the identity of the components is preserved, performance characteristics depend on size and shape of the component phases. The morphology in turn depends on interfacial and rheological properties of the components¹⁻⁴, but often to a similar extent on the processing conditions⁵⁻⁷.

Injection moulding is one of the most important processing techniques by which blends are fabricated into plastic parts; the morphological anisotropy characteristic of injection-moulded blends is primarily the result of orientation of phases along the complex melt flow lines during mould filling, which include the 'fountain flow' pattern at the melt front⁸. In this case, a very thin region of material at the mould surface experiences elongational flow at the front of the fountain flow pattern and creates an oriented surface skin. Most of the material has a melt morphology determined initially by shear and elongational flow fields experienced prior to entering the mould followed in the mould filling stage by shear flow behind the front of the fountain flow pattern. The shear rate profile through the thickness can create a gradient in the melt morphology. How much of the melt morphology is retained after cessation of flow depends on the cooling rate, which determines the amount of relaxation that occurs before solidification of the melt.

The mode of dispersion also depends on the interfacial properties of the components. In some cases, the interfacial energy between two unmodified polymers is sufficiently low that dispersion does not require a 'compatibilizing' agent and can be achieved by simply melt mixing the two polymers⁹⁻¹². Polycarbonate (PC) blended with acrylonitrile-butadiene-styrene (ABS) is an example of a system that is compatible in the practical sense that, when melt blended, the components are well dispersed with sufficient interfacial adhesion to realize significant property enhancement. In this study similar injection moulding conditions were used to prepare blends of PC and ABS that spanned the entire composition range in increments of 10 weight per cent. The morphology of injection-moulded pieces was characterized and subsequently described with the focus on processing-induced features that related to blend composition.

EXPERIMENTAL METHODS

Blends of ABS and PC were provided by The Dow Chemical Company in the form of 5 inch (12.7 cm) × 3 inch (7.6 cm) × 1/8 inch (0.3 cm) injection-moulded plaques. Samples were provided across the entire composition range in 10 wt% increments, and the compositions are indicated as the weight per cents PC/ABS. The ABS and PC resins were described previously¹³. For injection moulding, the melt temperature was 270°C for the PC-rich blends and 250°C for the ABS-rich blends; otherwise the moulding conditions were the same as described previously¹³.

*To whom correspondence should be addressed

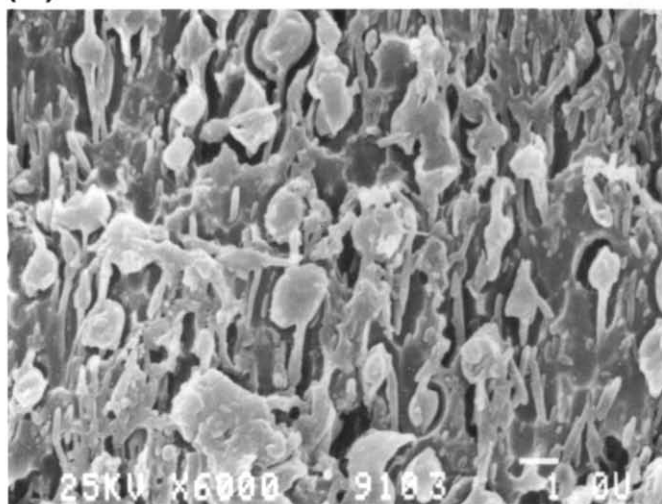
Tensile specimens were cut to the ASTM 1708 geometry either parallel or perpendicular to the injection direction. A single edge notch (SEN) was machined at the midpoint of the gauge length; the notch was 0.037 inch (0.094 cm) in depth with a 0.010 inch (0.025 cm) notch radius and 45° flank angle. The specimens were cut and notched in such a way that the location of the fracture surfaces would correspond to the midpoint of the plaque. The notched tensile specimens were fractured in the Instron at -70°C with a crosshead speed of 229 mm min^{-1} . The cryogenic fracture surfaces were subsequently selectively etched by immersion in 30% by weight aqueous potassium hydroxide for 2 to 5 h, dried, coated with gold and examined in the JEM 35CF scanning electron microscope (SEM)¹³. Alternatively, some of the etched specimens were stained with a 1 wt% aqueous solution of osmium tetroxide at room temperature for 1 week, then coated with gold and

examined in a JEOL 840A scanning electron microscope in the backscatter mode. Two of the blends, PC/ABS 50/50 and 30/70, were annealed in the d.s.c. nominally for 12 s at 250°C and then etched. The procedures were the same as described previously¹³.

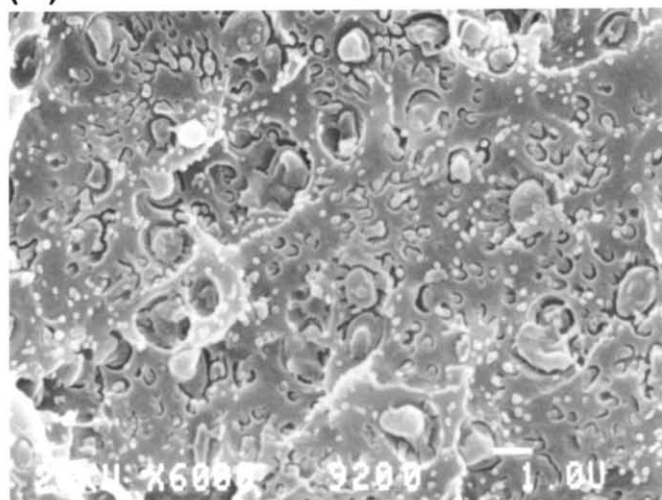
RESULTS AND DISCUSSION

The morphology of PC/ABS blends was examined across the entire composition range. In all cases, the morphology gradient produced by the flow pattern through the thickness of the plaque was characterized. Although the morphology probably also varied to some extent along the length and width of the plaque, this was not examined, and the midpoint of the plaque was chosen as a representative location to compare the morphologies of the various compositions. Brittle fracture surfaces both parallel and perpendicular to the injection direction were etched to remove the PC phase and viewed in the SEM.

(a) $d = 0.13\text{ mm}$



(b) $d = 0.13\text{ mm}$



(c) $d = 1.5\text{ mm}$

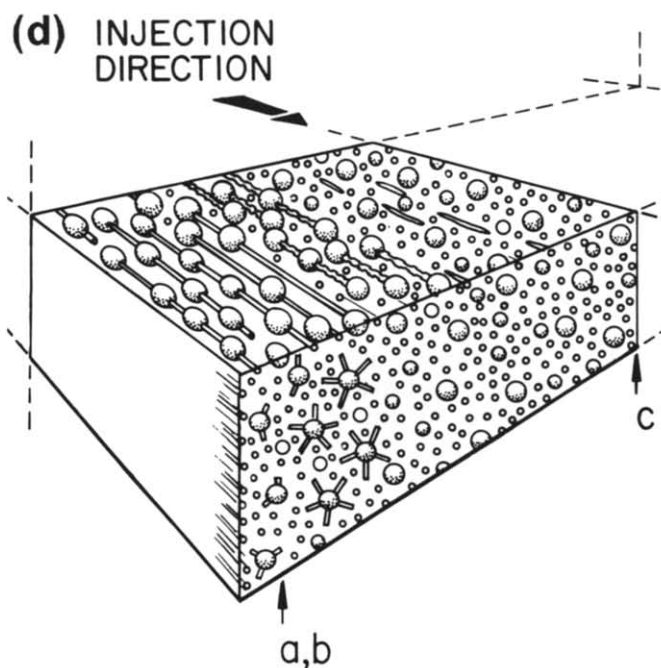
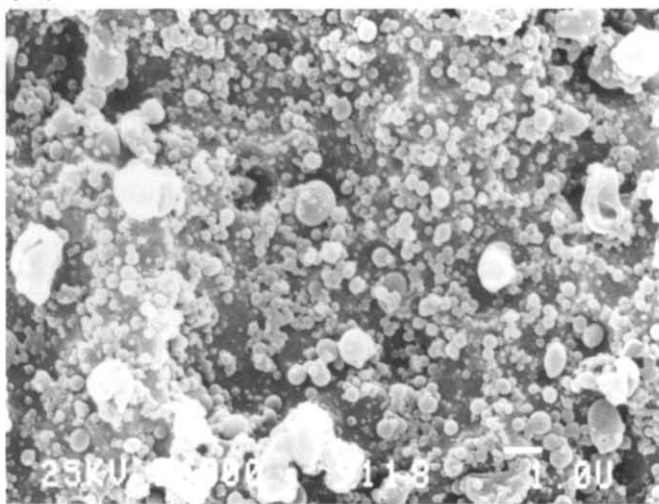


Figure 1 Scanning electron micrographs of injection-moulded PC/ABS 90/10 blend: (a) parallel to the injection direction near the edge; (b) perpendicular to the injection direction near the edge; (c) parallel to the injection direction at the centre; and (d) schematic representation of the morphology through the thickness. The distance d from the edge of the 3 mm thick plaque is indicated with each micrograph

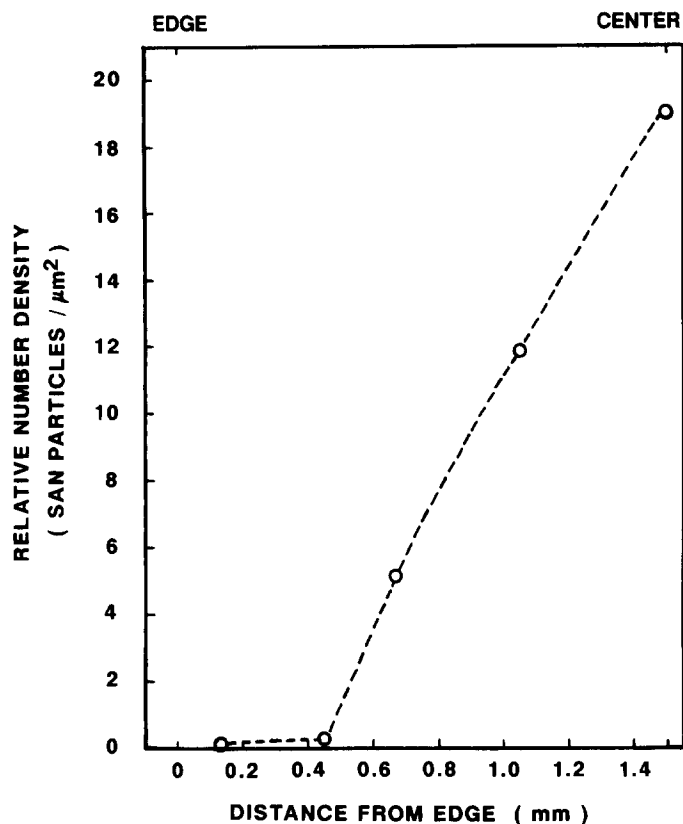


Figure 2 The relative number density of SAN particles on micrographs of a PC/ABS 90/10 parallel fracture surface at various positions through the thickness

The micrographs used to illustrate the various morphologies were at the same magnification, $6000\times$, in order to emphasize the changes that occurred as the composition was varied.

PC-rich compositions

PC/ABS 90/10. Near the edge of the PC/ABS 90/10 composition, the ABS phase had the 'bead-and-string' structure described previously¹³. Rubber particles connected by styrene-acrylonitrile (SAN) strings about 0.1 to $0.3\ \mu\text{m}$ in diameter and oriented in the injection direction created ABS bead-and-string domains that were essentially continuous in the injection direction (Figure 1a). Circular cross-sections and protruding ends of fractured SAN strings about $0.2\ \mu\text{m}$ in diameter were seen in the perpendicular fracture surface (Figure 1b). This view also showed star-like arrays with several SAN strings emanating from a rubber particle; these appeared to produce connections between bead-and-string structures. Near the centre of the plaque, the morphology appeared the same in both parallel and perpendicular directions. The ABS phase that remained when the PC was etched away consisted of two populations of dispersed spheres (Figure 1c). The larger $1\ \mu\text{m}$ spheres were single rubber particles with grafted SAN, while the free SAN was dispersed as the smaller $0.3\ \mu\text{m}$ spheres. Identification of the small spheres was confirmed when they were selectively removed by etching with acetone, a solvent for SAN, and the rubber particles were identified with the large spheres when SEM backscatter images showed the large spheres to be selectively stained by OsO_4 (ref. 13).

The gradient in morphology through the thickness of the PC/ABS 90/10 composition was determined by

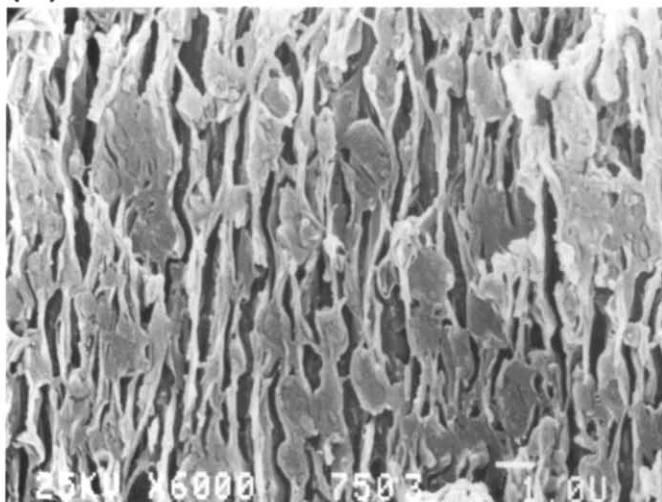
examining entire etched brittle fracture surfaces in both the parallel and perpendicular directions, and is shown schematically in Figure 1d. In the centre, large rubber particles and smaller free SAN particles were randomly dispersed in the PC matrix. Somewhat away from the centre, occasional rod-shaped SAN domains elongated in the injection direction appeared; closer to the edge, the SAN domains become longer and thinner and were frequently connected to rubber particles. This oriented bead-and-string structure was the dominant morphology of the ABS phase near the edge.

The gradient in morphology through the thickness was illustrated by determining the number density of SAN spheres on parallel micrographs from various positions. While the absolute numbers are not significant, the relative number density of free SAN particles plotted in Figure 2 shows that there were essentially no spherical particles near the edge, while at about $0.5\ \text{mm}$ in from the edge the number of free SAN particles began to increase rapidly and continued to increase to the centre.

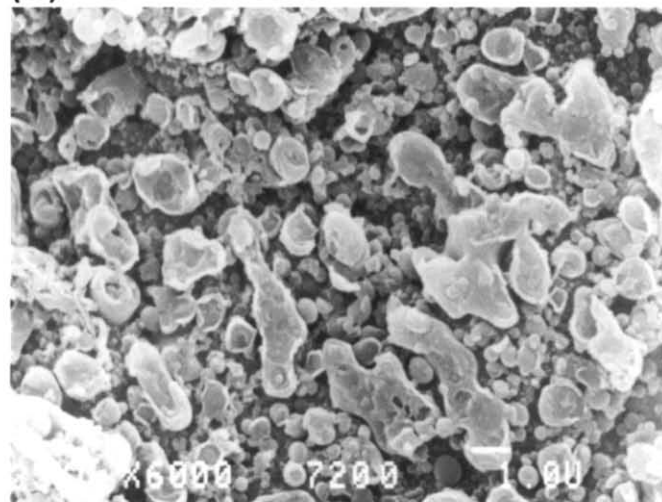
Formation of the bead-and-string structure during injection moulding of PC/ABS 90/10 blend was described in a previous publication¹³. Briefly, formation of the ABS bead-and-string morphology was thought to occur prior to entering the mould where the melt was subjected to elongational and shear flow, and in the mould where the flow pattern was fountain flow. The crosslinked rubber particles were not very deformable; however, since the viscosity of free SAN was lower than that of PC¹³, the free SAN would have been highly extended under elongational or shear flow conditions while miscibility with the grafted SAN would have provided adhesion to the rubber particles. Where the shear or elongational flow stresses were minimal, as during mould filling in the centre of the mould behind the fountain flow front, or when mould filling was completed, the highly drawn SAN strings would have had an opportunity to relax. The extent of relaxation would have depended on the shear rate profile through the thickness of the plaque, which determined the amount of elongation in the melt, and the cooling rate after mould filling, which controlled the amount of melt relaxation before solidification. Close to the mould contacting surface, the melt would have solidified rapidly and the solid-state morphology would most closely have resembled the melt morphology. In the centre of the plaque, the low shear rate during mould filling and longer cooling time after mould filling would have favoured relaxation of the bead-and-string morphology. Instead of relaxing to a composite ABS domain, Rayleigh instabilities, i.e. disturbances in the cross-section of the very long, thin SAN string, caused it to break up into a series of spherical SAN particles. In the centre of the plaque, the SAN spheres, separated from the rubber particles, and possessing a diameter on the same size scale as the diameter of the SAN strings, argued for the break-up mechanisms in this region.

PC/ABS 70/30. The bead-and-string structure was also observed near the edge of the plaque when the blend composition was PC/ABS 70/30. In the view parallel to the injection direction (Figure 3a), the bead-and-string structure was more dense than in the 90/10 composition and, although the SAN strings had approximately the same diameter, about $0.2\ \mu\text{m}$, there appeared to be

(a) $d = 0.18$ mm



(d) $d = 1.5$ mm



(b) $d = 0.22$ mm

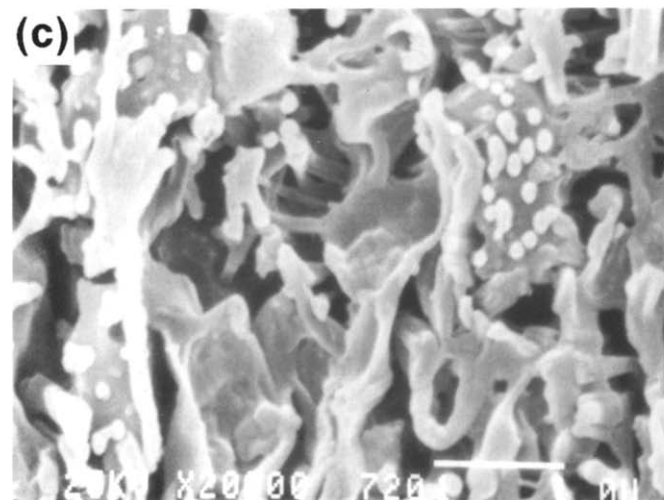
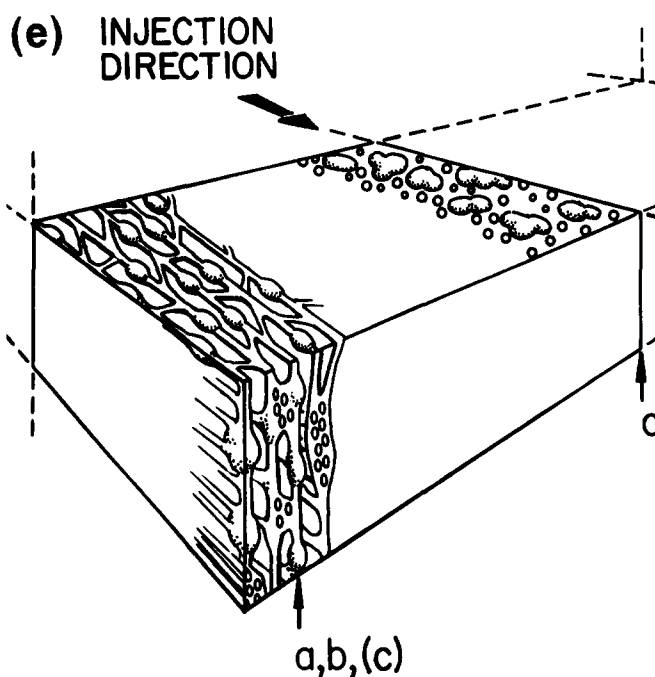
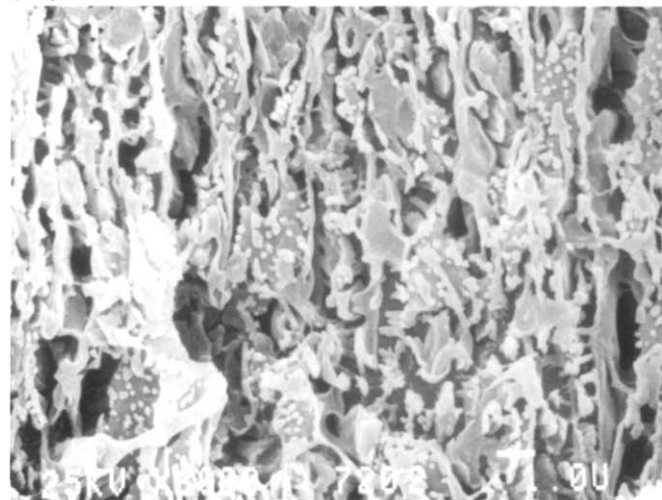


Figure 3 Scanning electron micrographs of injection-moulded PC/ABS 70/30 blend: (a) parallel to the injection direction near the edge; (b) perpendicular to the injection direction near the edge; (c) a higher magnification of (b); (d) parallel to the injection direction at the centre; and (e) schematic representation of the morphology through the thickness. The distance d from the edge of the 3 mm thick plaque is indicated with each micrograph

numerous interconnections between nearby bead-and-string structures. The perpendicular view contained many broken ends of SAN strings (Figure 3b) and, additionally, some small areas of coalescence were seen. The interconnections and coalescence of the bead-and-string structure were more apparent in a higher-magnification view perpendicular to the injection direction (Figure 3c). The rubber particle in the centre of the micrograph had

numerous SAN strings attached that interconnected with other SAN strings and nearby rubber particles. Just beside it, a group of SAN strings, seen in the micrograph as a cluster of broken ends, all appeared to emanate from a coalesced region.

The morphology of the ABS phase in the centre of the plaque consisted of dispersed rubber particles and smaller particles of free SAN. Compared with the 90/10

composition, the particles were more numerous, and, in addition, some irregularly shaped ABS domains that contained more than one rubber particle were in evidence (*Figure 3d*). Perpendicular views of the ABS morphology in the centre of the plaque were indistinguishable from *Figure 3d*; PC was clearly the continuous phase in this region of the plaque.

Coalescence of bead-and-string domains near the edge is shown schematically in *Figure 3e*. While the SAN is represented as being predominantly string-like in this region, as was apparent from the parallel views and the numerous broken ends in the perpendicular micrographs, the schematic drawing shows the initial stage in the formation of sheet-like ABS domains by coalescence and interconnect of bead-and-string structures. The process of coalescence by which a sheet-like morphology evolved from the bead-and-string structures as they become more densely arrayed was most apparent in cross-section, that is, in the perpendicular micrographs. Here, in addition to the ends of individual strings, elongated domains created by coalescence of several strings were visible. Some coalescence of SAN strings was also apparent in the parallel direction; coalescence in this view showed interconnections that gave the ABS phase a degree of continuity in the thickness direction.

The melt had an opportunity to relax in the centre of the mould during cooling. Melt relaxation by the break-up mechanism required long thin SAN strings, and the presence of numerous small $0.25\ \mu\text{m}$ SAN particles in the centre region was an indication that, despite the interconnections, many SAN strings or segments of strings were long enough to break up by the growth of Rayleigh instabilities. On the other hand, there were also larger composite ABS domains in the centre with several rubber particles such as might have formed by the relaxation of an interconnected or partially coalesced bead-and-string structure.

Intermediate blend compositions

PC/ABS 60/40. The morphology of the PC/ABS 60/40 blend composition, when viewed near the edge parallel to the injection direction, appeared very similar to the 70/30 composition with the ABS phase forming interconnected bead-and-string structures (*Figure 4a*). However, perpendicular to the injection direction, a typical view showed only occasional ends of SAN strings (*Figure 4b*); instead, the morphology of the ABS domains in the perpendicular view was very similar to that in the view parallel to the injection direction. Taken together, the two edge views (*Figures 4a* and *4b*) suggested a stratified, sheet-like ABS morphology that could have formed by lateral coalescence of the interconnected ABS bead-and-string domains. The formation of such a sheet-like domain by coalescence of numerous SAN strings was seen end-on in a higher-magnification perpendicular view (*Figure 4c*).

In the centre, the PC phase of the 60/40 composition was continuous with numerous dispersed rubber particles and free SAN spheres (*Figure 4d*); however, in addition, large irregularly shaped ABS domains were also present. These were highly branched and somewhat more extended in the injection direction than through the thickness. They created regions in which the ABS phase was co-continuous with PC. The morphology of the PC/ABS 60/40 blend as shown schematically in *Figure 4e* was significantly different from that of the

70/30 blend both near the edge, where the morphology of the 60/40 blend was clearly stratified rather than predominantly the linear bead-and-string structure, and in the centre, where there were regions of co-continuity of the phases in the 60/40 blend while the ABS phase clearly formed only inclusions in the 70/30 composition.

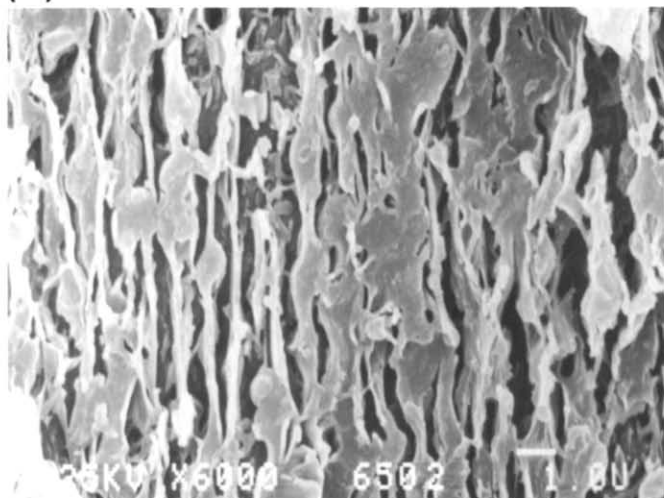
PC/ABS 50/50. The morphology of the 50/50 composition was examined in some detail as being representative of the intermediate composition range, 60/40 to 40/60. Etched brittle fracture surfaces of the PC/ABS 50/50 composition at four positions (*Figure 5*) illustrate the gradient in morphology through the thickness both parallel and perpendicular to the injection direction. Close to the edge, a view of the morphology parallel to the injection direction (*Figure 5a*) showed coalesced sheet-like ABS domains extended in the injection direction. Only occasionally could an isolated segment of the bead-and-string structure be found in the parallel micrographs.

Perpendicular to the flow, only a few broken ends of SAN strings were visible (*Figure 5b*); these had the same diameter, about $0.2\ \mu\text{m}$, as strings in the bead-and-string structure of the 90/10 composition. The predominant feature of the ABS phase in the perpendicular view was the elongated domain morphology that caused the perpendicular view to resemble closely the parallel view in appearance, and revealed that the ABS domain morphology was sheet-like near the edge. Upon careful examination, the ABS domains appeared more coalesced in the parallel view, while in the perpendicular view evidence remained of the bead-and-string structure. In particular, many of the ABS domains had numerous strings attached. This suggested that during flow the bead-and-string structures became stratified and the interconnected SAN strings coalesced laterally to create the elongated appearance in the perpendicular direction. The PC domains were identified by the elongated holes that separated the ABS domains in both the parallel and perpendicular directions. Although the holes were somewhat more elongated in the perpendicular view, the PC phase also took on a sheet-like morphology near the edge of the plaque.

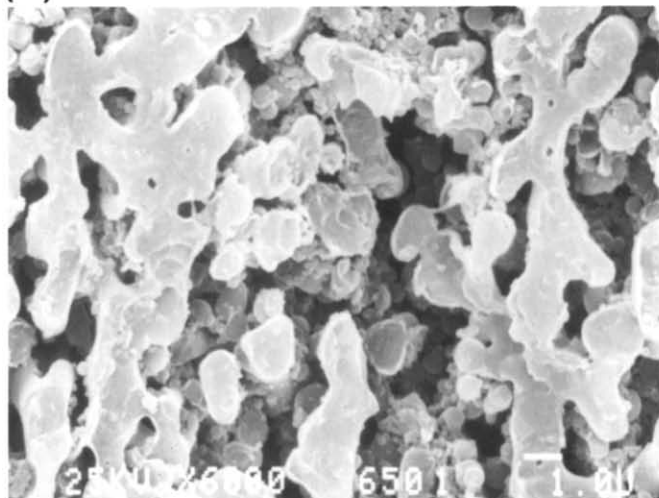
About $0.84\ \text{mm}$ inward from the edge, the ABS domains lost some of the sheet-like appearance (*Figure 5c*), especially in the perpendicular view (*Figure 5d*), and the holes that identified the PC domains were less extended in the injection direction. These were changes that might have occurred if the sheet morphology had just begun to relax before solidification; there was still evidence that this morphology derived from the bead-and-string structure, for example the occasional broken ends of SAN strings in the perpendicular view.

The morphology changed considerably at a depth of $1.27\ \text{mm}$ (*Figures 5e* and *5f*). The thin SAN strings observed near the edge were absent, and the stratified morphology was replaced by a thicker, interconnected ABS domain morphology that was continuous. The PC phase may also have been continuous. The micrographs showed irregular elongated holes as well as circular holes created when the PC was etched away. While these holes could have indicated discrete domains, they could also have been connected to create a continuous interpenetrating PC phase. Parallel and perpendicular views were similar. In lower-magnification views it was apparent that both parallel and perpendicular to the

(a) $d = 0.19$ mm



(d) $d = 1.5$ mm



(b) $d = 0.21$ mm

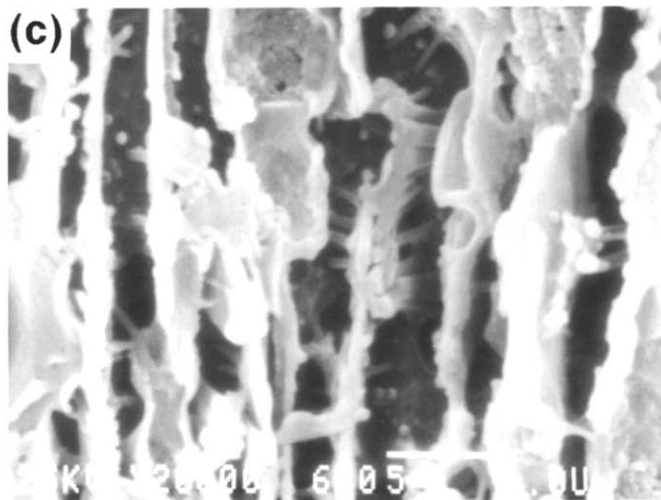
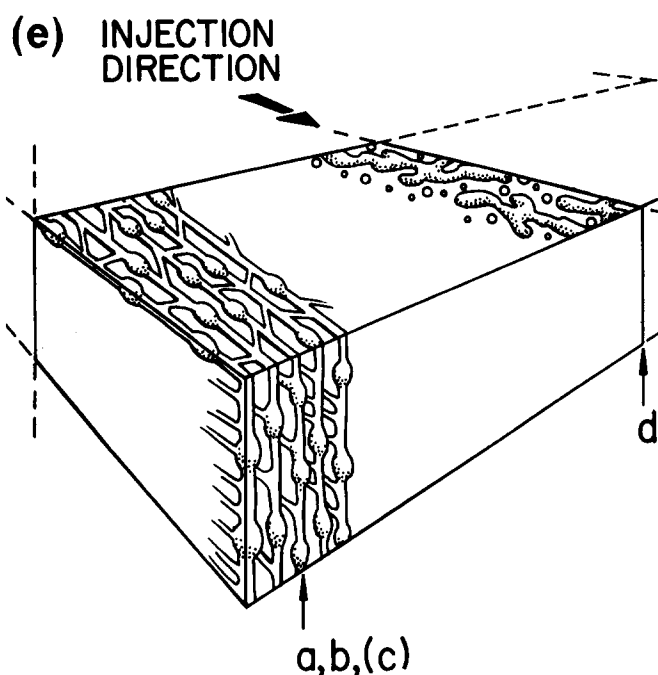
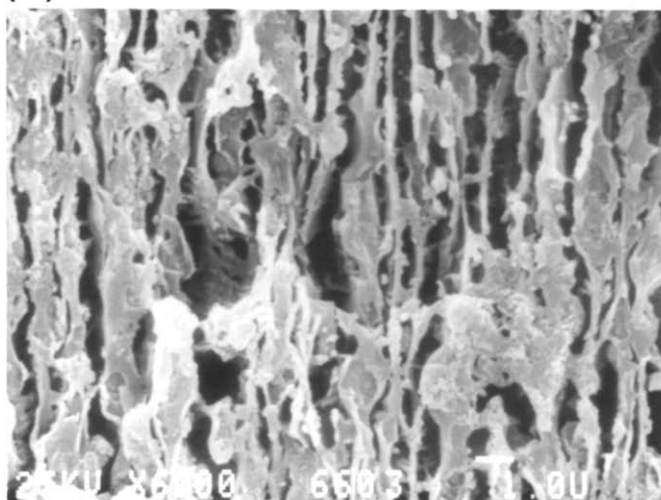


Figure 4 Scanning electron micrographs of injection-moulded PC/ABS 60/40 blend: (a) parallel to the injection direction near the edge; (b) perpendicular to the injection direction near the edge; (c) a higher magnification of (b); (d) parallel to the injection direction at the centre; and (e) schematic representation of the morphology through the thickness. The distance d from the edge of the 3 mm thick plaque is indicated with each micrograph

injection direction the PC and ABS domains were more extended in the plane of the plaque than in the thickness direction.

Further changes in the morphology from a depth of 1.27 mm (Figures 5e and 5f) to the centre (Figures 5g and 5h) were only slight. Both ABS and PC domains were somewhat thicker in the centre and directionality of the morphology was less apparent. Both parallel and

perpendicular views near the centre showed numerous small SAN spheres remaining in the holes where the PC was etched out. These spheres were the same size, about $0.2 \mu\text{m}$ in diameter, as the SAN spheres observed in the PC-rich blends.

One approach to quantifying the coarseness of a phase morphology uses the Chalkley method to estimate the volume-to-surface ratio from micrographs^{14,15}. A line of

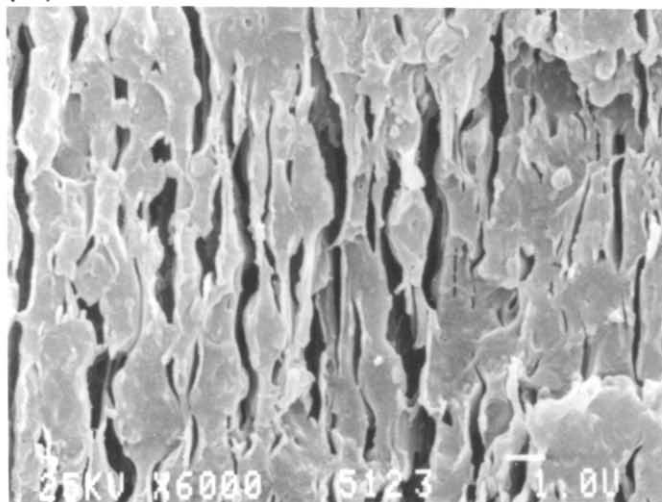
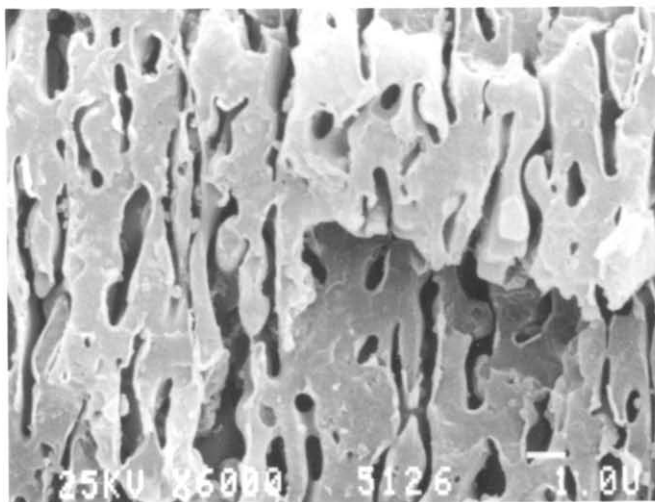
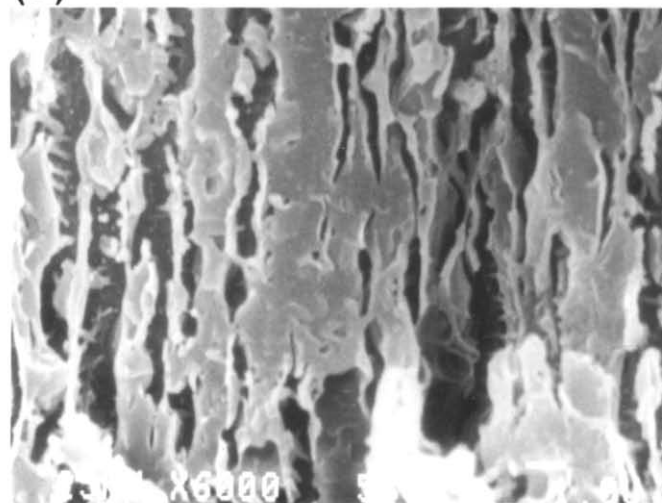
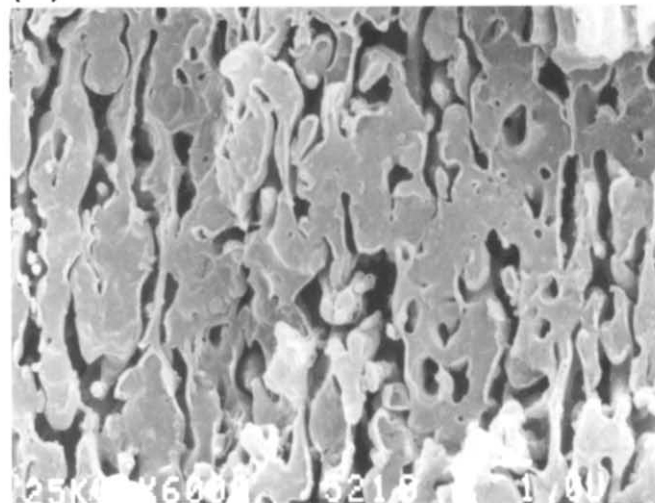
(a) $d = 0.26$ mm(c) $d = 0.84$ mm(b) $d = 0.21$ mm(d) $d = 0.84$ mm

Figure 5 Scanning electron micrographs of injection-moulded PC/ABS 50/50 blend at various positions through the thickness: (a), (c), (e) and (g) parallel to the injection direction; and (b), (d), (f) and (h) perpendicular to the injection direction. The distance d from the edge of the 3 mm thick plaque is indicated with each micrograph

length l is placed randomly on an SEM micrograph and the number of hits N_h , defined as the number of times the end fell inside the phase of interest, in this case a PC domain, and the number of cuts N_c , the number of times the line crossed an interface, are determined. The Chalkley parameter C then gives the ratio of volume to surface according to:

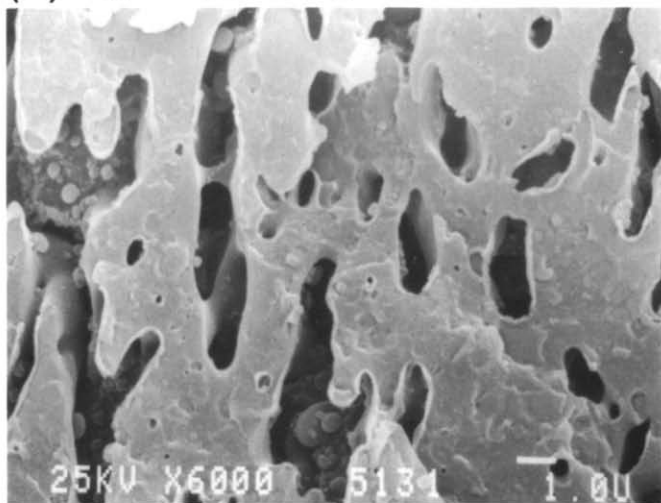
$$C = lN_h/4N_c \quad (1)$$

and the reciprocal Chalkley parameter C^{-1} is an estimation of the average surface per unit volume. The reciprocal Chalkley parameter for the PC phase was determined from the parallel views of the morphology at various locations through the thickness with $l = 10 \mu\text{m}$, and when plotted as a function of location (*Figure 6*) clearly revealed the change in morphology through the thickness. The reciprocal Chalkley parameter was largest at the edge where the thin sheet-like domains created a large surface-to-volume ratio. It decreased from a value of 11 at the edge to 2.5 in the centre with most of the decrease occurring about midway to the centre at the position where the change from thin sheet-like domains

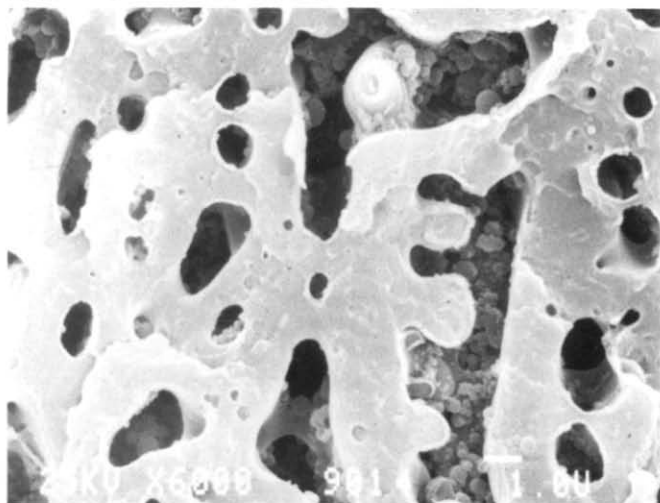
to thicker interconnected ABS domains with a lower surface-to-volume ratio was noted in the micrographs.

A schematic model of the gradient morphology through the thickness of the PC/ABS 50/50 blend was developed (*Figure 7*). The stratified, sheet-like morphology observed close to the mould surface where solidification would have occurred most rapidly was thought to represent most closely the morphology in the flowing melt. The phase separation of ABS itself gave an additional aspect of complexity to the morphology of the ABS phase in blends with PC. Taking the basic morphology of the ABS phase during melt flow to be the bead-and-string structure, the sheet-like morphology of the 50/50 blend was viewed as the result of increasing interconnection, coalescence and stratification of the bead-and-string structure as the blend composition became richer in ABS. While the melt morphology was preserved to an extent by rapid cooling near the edge, considerable relaxation occurred in approximately the centre half of the thickness. Two mechanisms for relaxation of the ABS phase appeared to create the morphology in the centre region of the 50/50 blend

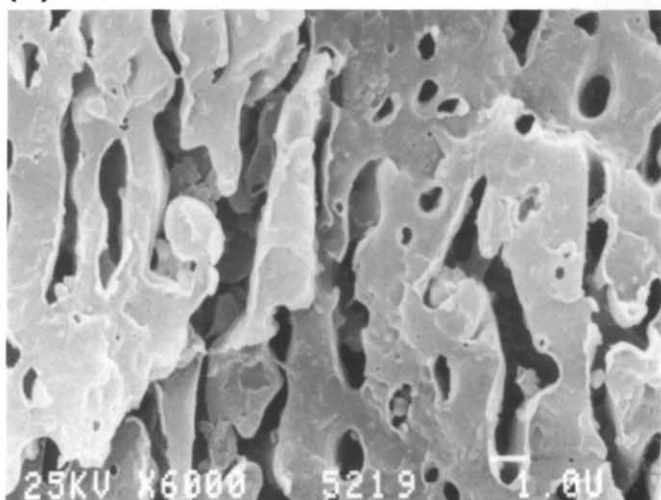
(e) $d = 1.27 \text{ mm}$



(g) $d = 1.5 \text{ mm}$



(f) $d = 1.29 \text{ mm}$



(h) $d = 1.5 \text{ mm}$

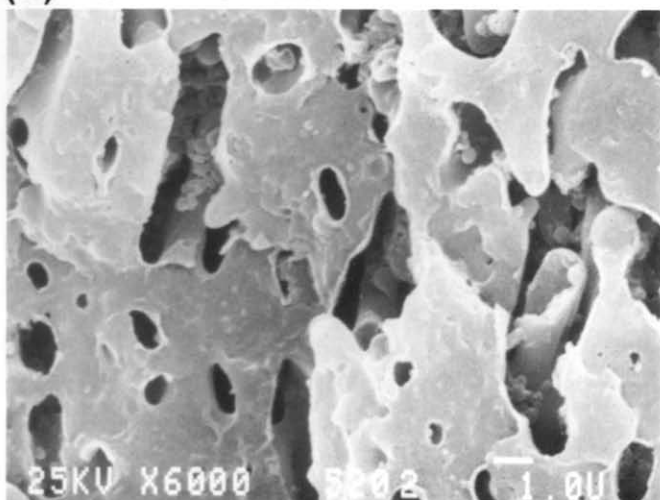


Figure 5 (continued)

composition. In PC-rich regions of the melt where the bead-and-string structure was not highly interconnected, break-up of long thin SAN strings created the $0.3 \mu\text{m}$ SAN particles that were observed at the two positions closest to the centre. However in regions where the bead-and-string structure was more coalesced, recovery into thick ABS domains would have been favoured. The thick continuous or semi-continuous ABS domains first appeared in the centre of the plaque when the ABS morphology at the edge was predominantly interconnected and stratified.

Previously, it was demonstrated that relaxation of the bead-and-string structure created the small SAN spheres by the Rayleigh instability mechanism when intermediate stages of break-up were observed after the bead-and-string structure was annealed for short periods of time in the d.s.c.¹³ Relaxation of the interconnected, stratified ABS morphology was examined in the same way. After the initial interconnected, stratified morphology near the edge (Figure 8a) was heated to 250°C for only about 12 s, the stratification was much less apparent (Figure 8b) while the ABS domains had become thicker and appeared to be sufficiently interconnected that the ABS phase was

continuous. Occasionally, thin SAN strings in various stages of break-up could also be seen in the micrographs of the annealed blend (arrows in Figure 8b), attesting to the role of both relaxation mechanisms in creating the morphology in the centre region of the intermediate blend compositions.

PC/ABS 40/60. Near the edge of the 40/60 composition the interconnected ABS bead-and-string structures were densely arrayed and interspersed with elongated PC domains (Figure 9a). Viewed in the parallel direction near the edge, the only noticeable change through the intermediate composition range, PC/ABS 60/40 to 40/60, was progressively more coalescence of the ABS bead-and-string structure. Particularly in the perpendicular view (Figures 9b and 9c) there was evidence that a network of SAN strings had coalesced to create the stratified morphology, but overall the views parallel and perpendicular to the injection direction were very similar. The similarity in the parallel and perpendicular views near the edge, and the stratified, sheet-like morphology these revealed, were distinguishing

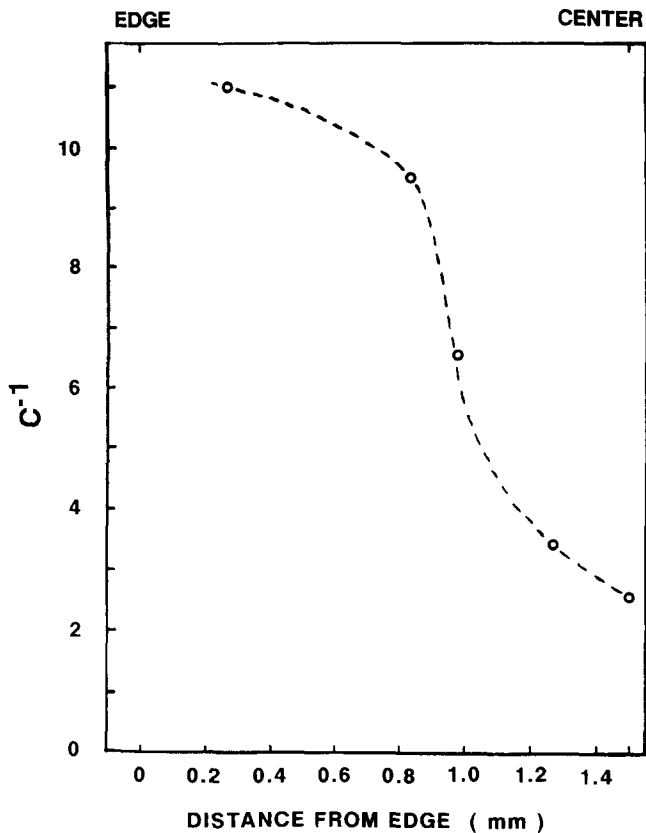


Figure 6 The reciprocal Chalkley parameter C^{-1} through the thickness of the PC/ABS 50/50 blend

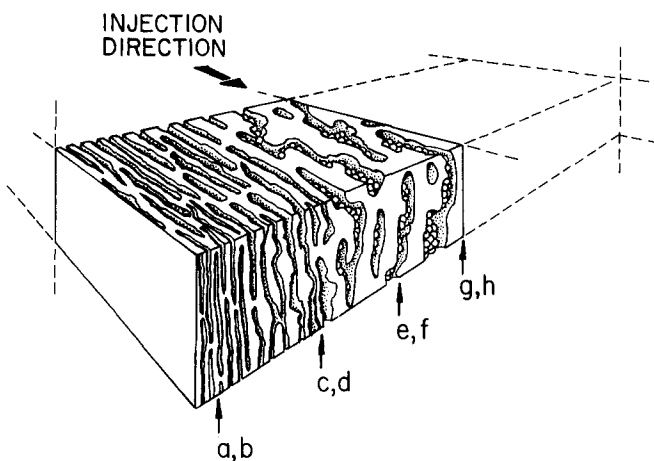


Figure 7 Schematic representation of the morphology of the PC/ABS 50/50 blend

features that differentiated the intermediate blend compositions from the PC-rich compositions.

In the centre of the plaque the ABS phase was continuous (Figure 9d). The morphology appeared the same in both parallel and perpendicular directions with irregularly shaped PC domains identified by the holes. In this view the PC phase did not appear to be co-continuous with the ABS although in places the PC domains were interconnected over short distances. Most of the holes left when the PC was etched away contained spherical SAN particles about $0.2 \mu\text{m}$ in diameter. The presence of SAN inclusions in the PC domains probably resulted from the break-up of isolated SAN strings in PC-rich regions of the melt, although it has also been

suggested that composite domains can exist in the flowing melt¹⁶. The morphology of the PC/ABS 40/60 blend is shown schematically in Figure 9e. A distinguishing feature of the intermediate composition range, PC/ABS 60/40 to 40/60, was the continuous or semi-continuous nature of the ABS phase in the centre; this was thought to result from relaxation of the stratified, sheet-like morphology that existed in the melt. The melt morphology was retained to a greater degree near the edge where the cooling rate was most rapid.

ABS-rich blend compositions

PC/ABS 30/70. The holes near the edge of etched brittle fracture surfaces of the PC/ABS 30/70 composition revealed PC domains less than $1 \mu\text{m}$ in diameter and elongated in the injection direction (Figure 10a). Perpendicular to the injection direction (Figure 10b) the holes were circular with a diameter corresponding to the width of the elongated holes in the parallel view. Sometimes, especially close to the edge, the holes in the perpendicular view were somewhat elongated, suggesting that the PC domains were sheet-like as well as rod-shaped in this region. In the centre (Figure 10c) the morphology was isotropic with spherical holes about $1 \mu\text{m}$ or less in diameter. The schematic model of the phase morphology (Figure 10d) showed the more-or-less isotropic morphology in the centre with spherical PC domains $1 \mu\text{m}$

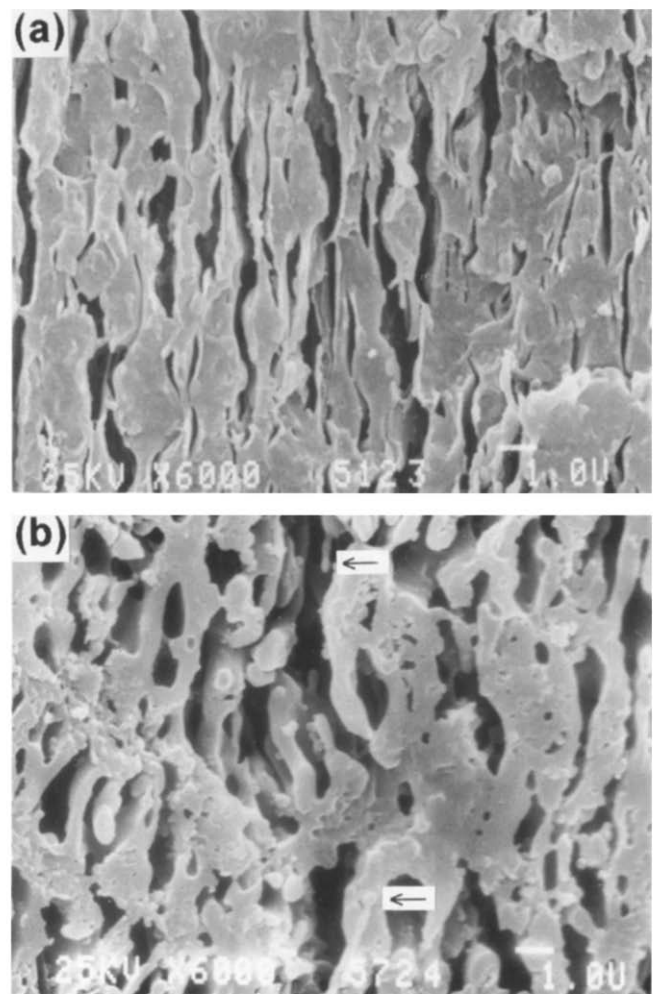
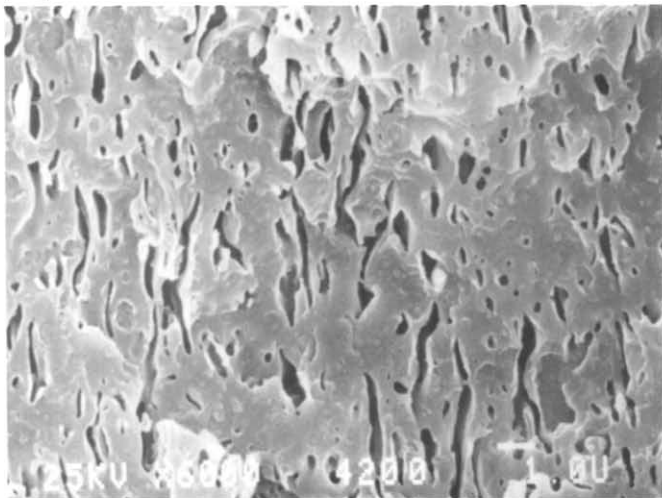
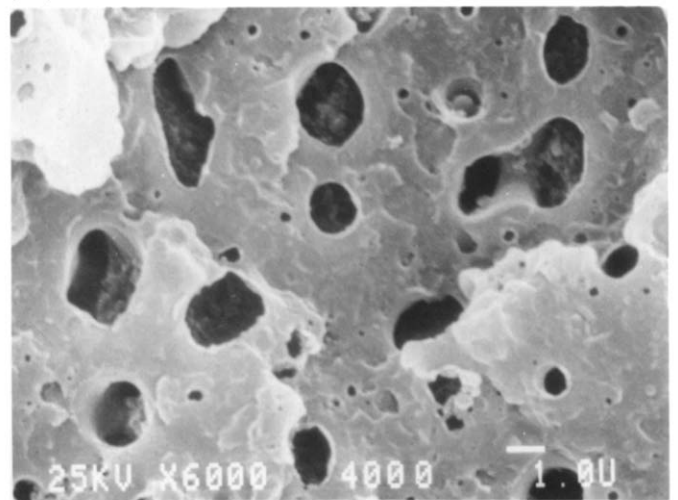


Figure 8 The annealed PC/ABS 50/50 blend viewed parallel to the injection direction near the edge: (a) the unannealed control; and (b) annealed for nominally 12 s at 250°C

(a) $d = 0.16$ mm



(d) $d = 1.5$ mm



(b) $d = 0.14$ mm

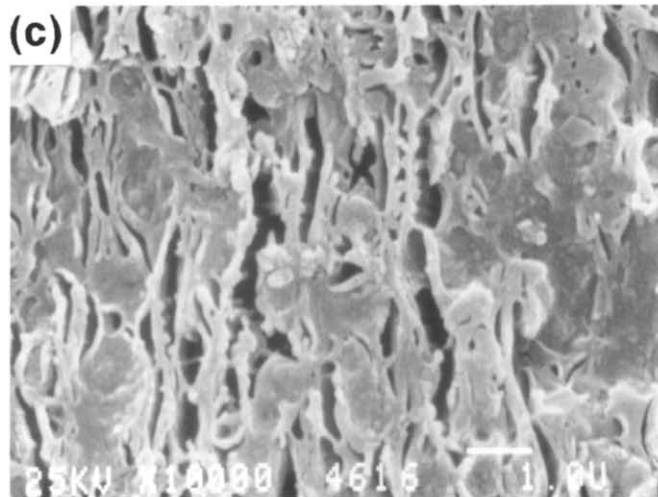
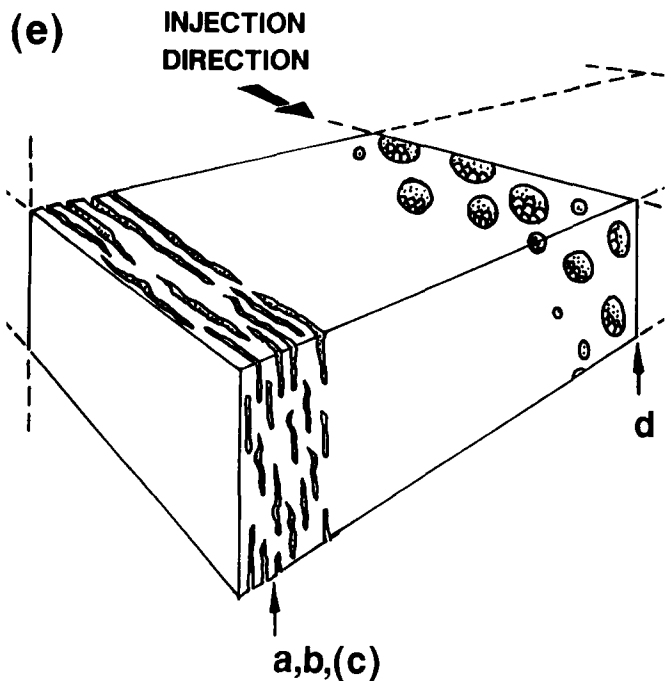
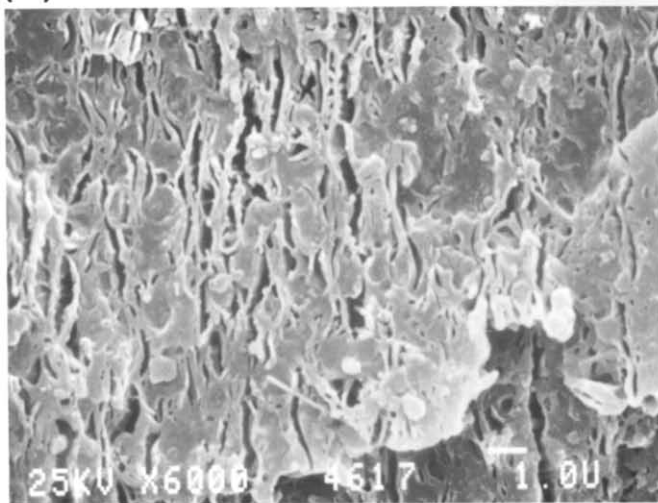


Figure 9 Scanning electron micrographs of injection-moulded PC/ABS 40/60 blend: (a) parallel to the injection direction near the edge; (b) perpendicular to the injection direction near the edge; (c) a higher magnification of (b); (d) parallel to the injection direction at the centre; and (e) schematic representation of the morphology through the thickness. The distance d from the edge of the 3 mm thick plaque is indicated with each micrograph

and less in diameter dispersed in the ABS matrix, while towards the edge the PC domains became elongated in the injection direction and took on a rod or sheet-like shape.

The length-to-width ratio of the PC domains (Figure 11) shows the change in shape through the thickness. The gradient in aspect ratio depended on the flow profile through the thickness, which determined the

amount of elongation in the melt, and the cooling rate after mould filling, which controlled the amount of melt relaxation. Since the melt viscosity of PC was greater than that of free SAN¹³, the PC domains were not as highly extended in the melt as the SAN was when ABS was the dispersed phase. Specifically, the PC domains were not so highly extended that they would have become unstable and broken up during relaxation as the SAN

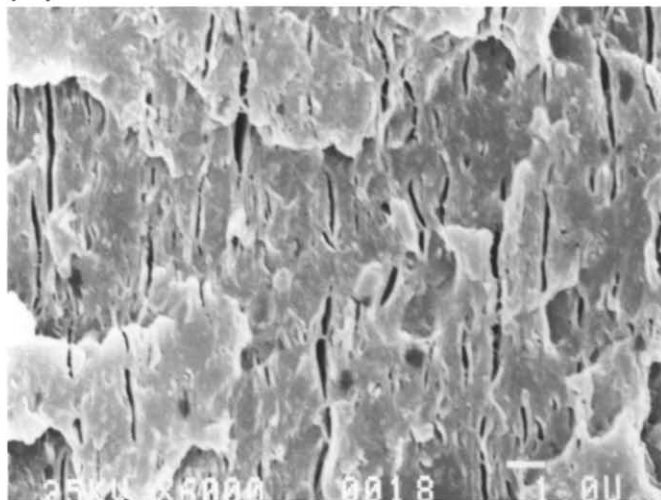
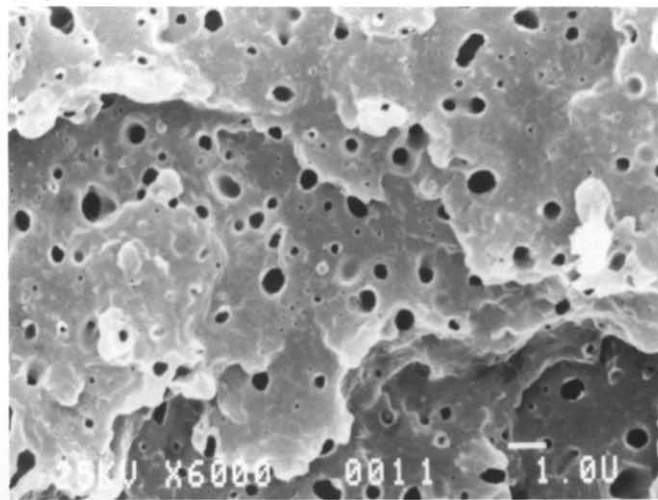
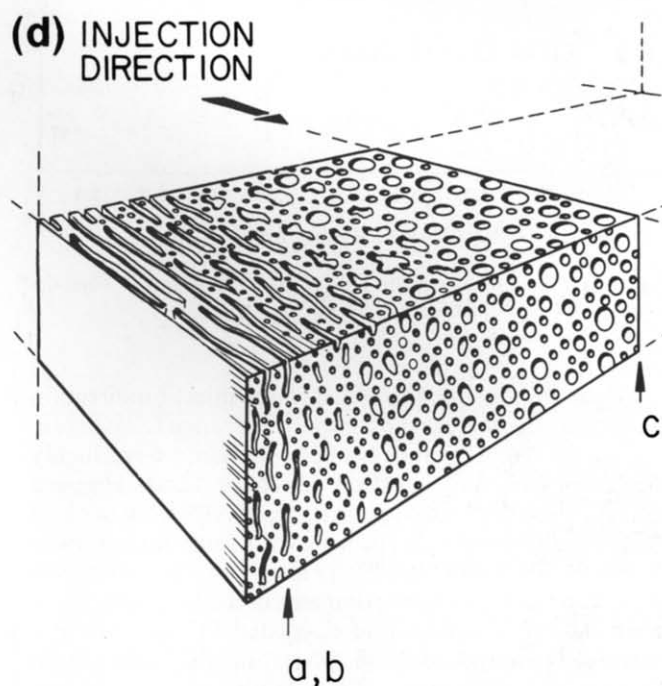
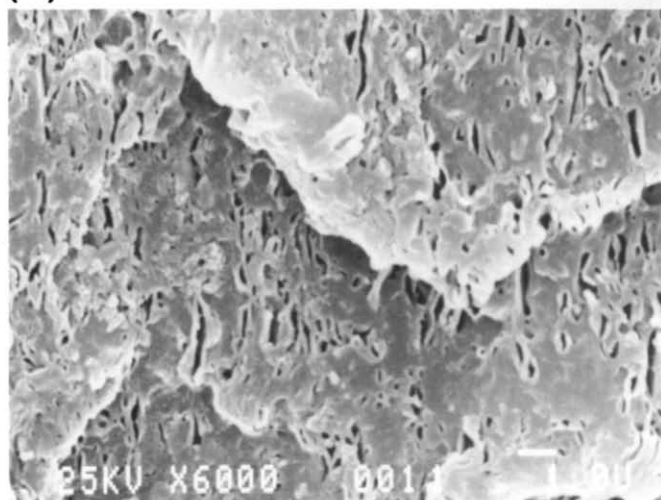
(a) $d = 0.12$ mm(c) $d = 1.5$ mm(b) $d = 0.11$ mm

Figure 10 Scanning electron micrographs of injection-moulded PC/ABS 30/70 blend: (a) parallel to the injection direction near the edge; (b) perpendicular to the injection direction near the edge; (c) parallel to the injection direction at the centre; and (d) schematic representation of the morphology through the thickness. The distance d from the edge of the 3 mm thick plaque is indicated with each micrograph

did. Instead, when elongational or shear flow ceased, the elongated PC domains would have relaxed to a spherical shape¹⁷. This was confirmed when the elongated domain morphology near the edge (*Figure 12a*) was replaced by a dispersion of spherical PC domains after the blend was annealed for nominally 12 s at 250°C (*Figure 12b*).

PC/ABS 10/90. The morphology of the PC/ABS 10/90 composition was similar to that of the 30/70 composition except that the elongated PC domains near the edge were shorter and thinner (*Figure 13a*) and the spherical domains in the centre were smaller (*Figure 13b*). The ABS-rich blends presented a conventional situation with regard to blend morphology. The decrease in domain size with decreasing concentration of the dispersed component, in this case the spherical PC domains in the centre decreased from an average diameter of 0.4 μm in PC/ABS 30/70 to 0.15 μm in 10/90, has been well documented¹⁸.

Effects of composition

A common feature of the injection-moulded plaques of all the PC/ABS blend compositions was the identification from the morphology gradient through the thickness of two fairly distinct zones. An edge zone extended approximately half the distance to the centre; here the morphology was strongly influenced by flow conditions during mould filling with domain morphologies that were highly extended in the injection direction. A second zone that comprised the centre half of the thickness showed minimal effects of mould filling flow; here the domain morphology possessed little or no directional variation and had an overall appearance that has been described in the literature as relaxed or coarsened. Because the morphologies of seven blend compositions spanning the entire composition range were characterized in some detail, it was possible to identify qualitatively systematic effects of composition on morphology of the edge and centre zones.

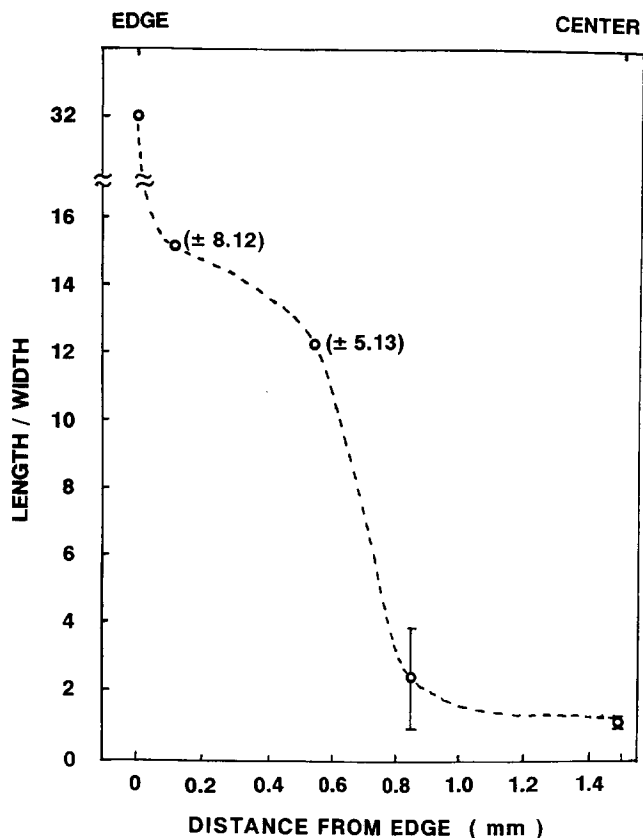


Figure 11 The length-to-width ratio of the PC domains through the thickness of the PC/ABS 30/70 blend

When the edge views parallel to the injection direction were compared across the composition range (Figures 1a, 3a, 4a, 5a, 9a, 10a and 13a) the domains were highly elongated in the injection direction and changed gradually as the blend became richer in ABS from isolated ABS bead-and-string structures with some interconnections in PC/ABS 90/10 (Figure 1a), to stratified, coalesced bead-and-string domains of the PC/ABS 50/50 composition (Figure 5a), to elongated PC domains in a completely coalesced ABS phase in PC/ABS 10/90 (Figure 13a). The views perpendicular to the injection direction were more revealing of the morphological changes that occurred in the edge zone with composition (Figures 1b, 3b, 4b, 5b, 9b, 10b and 13b). In the PC-rich blends, PC/ABS 90/10 and 70/30, free SAN was dispersed primarily as strings connecting rubber particles. This was inferred from the preponderance of circular cross-sections and broken ends of SAN strings in the perpendicular views of these compositions; only small areas where SAN strings had coalesced were observed. Coalescence of SAN strings into domains that persisted for large distances in the perpendicular view, with few cross-sections of SAN strings visible, was a major difference between the morphologies of the 70/30 and 60/40 compositions. As the blend was made increasingly rich in ABS, the coalesced, stratified ABS domains in the perpendicular view gradually thickened until ABS became the continuous phase in the ABS-rich blends.

The melt morphology during mould filling was only stable in flow, and the extent to which it was preserved near the edge was due to rapid cooling and solidification in this region of the mould. In the centre, considerable relaxation occurred either because of the slower cooling rate in this region and/or because the melt morphology

in this region was subjected to lower shear stresses during mould filling. It has been seen that the bead-and-string structure relaxed by growth of Rayleigh instabilities to a dispersion of individual rubber particles and SAN spheres. This was the primary relaxation mechanism in PC-rich blends and created a morphology in the centre where PC was the continuous phase. The break-up mechanism required long thin SAN strings. Even in the intermediate composition range, break-up of occasional SAN strings in PC-rich regions of the melt was probably the reason the PC domains in the centre contained some dispersed SAN spheres.

A second relaxation mode occurred when the stratified ABS morphology replaced the interconnected bead-and-string structure near the edge. When the bead-and-string structure coalesced and became stratified in the melt, relaxation into thick ABS domains replaced the break-up mechanism. Accordingly, the appearance of thick semi-continuous or continuous ABS domains in place of dispersed rubber and SAN particles in the centre coincided with the appearance of a stratified morphology near the edge, as revealed by the perpendicular edge views. This transition occurred at a blend composition of PC/ABS 60/40, and the second mode of relaxation predominated in all the intermediate compositions where the stratified, sheet-like ABS morphology was observed near the edge.

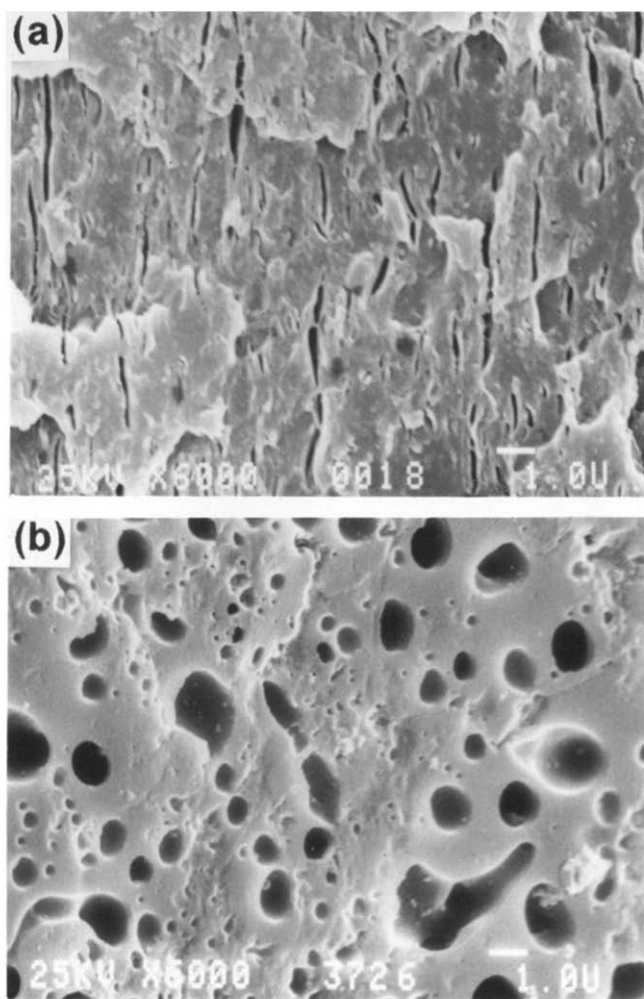


Figure 12 The annealed PC/ABS 30/70 blend viewed parallel to the injection direction near the edge: (a) the unannealed control; and (b) annealed for nominally 12 s at 250°C

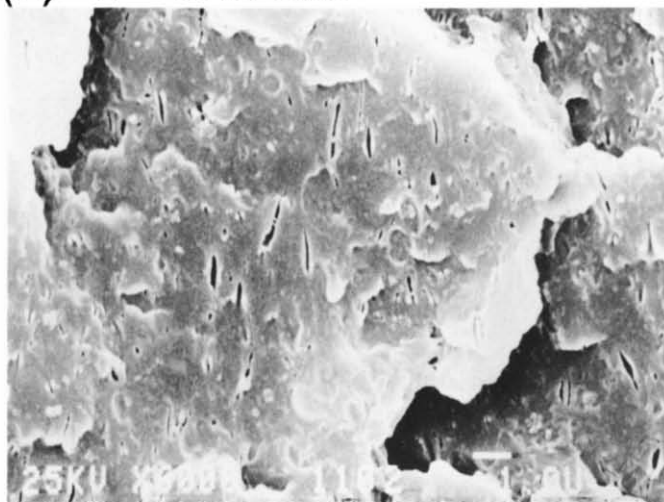
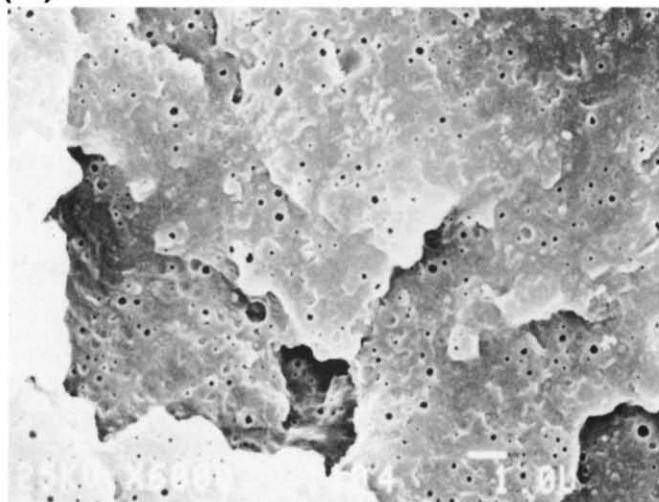
(a) $d = 0.15$ mm(b) $d = 1.5$ mm

Figure 13 Scanning electron micrographs of injection-moulded PC/ABS 10/90 blend: (a) parallel to the injection direction near the edge; and (b) parallel to the injection direction at the centre. The distance d from the edge of the 3 mm thick plaque is indicated with each micrograph

When the blend became richer in ABS, PC/ABS 30/70 and 10/90, dispersed PC domains were not so highly extended that they would have become unstable and broken up as the ABS bead-and-string structure did in the PC-rich blends. Consequently, only relaxation of extended PC domains was observed in the ABS-rich blends, and the morphology in the centre showed a gradual change from co-continuous ABS and PC phases to continuous ABS phase with dispersed PC as the composition changed from PC/ABS 50/50 to 10/90.

CONCLUSIONS

The morphology gradient of PC/ABS blends in injection-moulded plaques was characterized over the entire composition range. Examination of etched brittle fracture surfaces in the SEM through the thickness of the plaques led to the identification of three composition ranges based on the morphological features.

The PC-rich blends consisted of the composition range PC/ABS 90/10 to 70/30. The ABS phase formed bead-and-string structures near the edge of the plaque that were essentially continuous in the injection direction; with increasing ABS content, the bead-and-string structures became more densely arrayed and more interconnected. In the centre, PC was the continuous phase with ABS dispersed as individual rubber particles about $1 \mu\text{m}$ in diameter and smaller $0.3 \mu\text{m}$ particles of free SAN. When the ABS content was in the higher end of the range, some consolidated ABS domains were also observed.

There was a transition in the morphology between the PC/ABS 70/30 and 60/40 compositions. Intermediate compositions, 60/40 to 40/60, were characterized near the edge by an interconnected, coalesced ABS bead-and-string structure that with the PC phase formed a stratified sheet-like morphology. In the centre, the ABS phase appeared to be continuous. The PC phase was thought

to be co-continuous in the 60/40 composition, but formed a dispersed phase with SAN inclusions in the 40/60 composition.

The ABS-rich blends in the composition range PC/ABS 30/70 to 10/90 had a very conventional blend morphology with PC domains dispersed in the continuous ABS phase. The PC domains were elongated in the injection direction near the edge and were spherical in the centre of the plaque. The PC domains became smaller as the fraction of PC in the blend decreased.

ACKNOWLEDGEMENTS

Helpful discussions with Dr Che-I Kao and Dr Clive Bosniak of The Dow Chemical Company are gratefully acknowledged. Financial support for this research was provided by The Dow Chemical Company.

REFERENCES

- 1 Plochocki, A. P. *Polym. Eng. Sci.* 1983, **23**, 618
- 2 Karger-Kocsis, J., Kalló, A. and Kuleznev, Y. N. *Polymer* 1984, **25**, 279
- 3 Howe, D. V. and Wolkowicz, M. D. *Polym. Eng. Sci.* 1987, **27**, 1582
- 4 Wu, S. *Polym. Eng. Sci.* 1987, **27**, 335
- 5 Karger-Kocsis, J. and Csikai, I. *Polym. Eng. Sci.* 1987, **27**, 241
- 6 Thamm, R. C. *Rubber Chem. Tech.* 1977, **50**, 24
- 7 White, J. L. and Dietz, W. *Polym. Eng. Sci.* 1979, **19**, 1081
- 8 Tadmor, Z. *J. Appl. Polym. Sci.* 1974, **18**, 1753
- 9 Kurauchi, T. and Ohta, T. *J. Mater. Sci.* 1984, **19**, 1699
- 10 Kim, W. N. and Burns, C. M. *Polym. Eng. Sci.* 1988, **28**, 1115
- 11 Suarez, H., Barlow, J. W. and Paul, D. R. *J. Appl. Polym. Sci.* 1984, **29**, 3253
- 12 Stefan, D. and Williams, H. L. *J. Appl. Polym. Sci.* 1974, **18**, 1451
- 13 Lee, M. P., Hiltner, A. and Baer, E. *Polymer* 1992, **33**, 0000
- 14 Chalkley, H. W., Cornfield, J. and Park, H. *Science* 1949, **110**, 295
- 15 Quintens, D., Groeninckx, G., Guest, M. and Aerts, L. *Polym. Eng. Sci.* 1991, **31**, 1207, 1215
- 16 Vanoene, M. J. *Colloid Interface Sci.* 1972, **40**, 448
- 17 Stone, H. A. and Leal, L. G. *J. Fluid Mech.* 1989, **198**, 399
- 18 Heikens, D. and Barentsen, W. *Polymer* 1977, **18**, 69